JCTC Journal of Chemical Theory and Computation

Quantum Chemical Characterization of the Structural and Energetic Properties of HCN−BF_3

James A. Phillips*,† and Christopher J. Cramer‡

Department of Chemistry, University of Wisconsin−Eau Claire, 105 Garfield Avenue, Eau Claire, Wisconsin 54701, and Department of Chemistry and Supercomputer Institute, University of Minnesota, 207 Pleasant Street SE, Minneapolis, Minnesota 55455

Received May 3, 2005

Abstract: The structure, dipole moment, binding energy, and vibrational frequencies of HCN−BF_3 are investigated via 12 DFT methods as well as MP2, MC-QCISD, and MCG3 calculations. By comparing the DFT results to both experimental data and results from post-Hartree−Fock molecular orbital methods, we gauge the effectiveness of various density functionals in modeling this fairly weak donor−acceptor system. For structural data, B3PW91, B98, and *m*PWPW91 provide results that compare favorably with experiment. All DFT methods that yield a reasonable structure predict dipole moments that are only slightly larger than the experimental value by 0.1 to 0.2 D. Moreover, to ensure that a comparison of calculated (equilibrium) and experimental (vibrationally averaged) data is indeed valid for this system, the B−N distance potential is calculated using B3PW91, MP2, and MCG3, and the one-dimensional Schrödinger equation for motion along this bond-stretching coordinate is solved to obtain vibrational energy levels, wave functions, and expectation values of the B−N distance and dipole moment. In every instance, average bond lengths differ by only a few thousandths of an angstrom from the corresponding equilibrium values, and dipole moments are unchanged to within hundredths of a debye. For vibrational frequencies, B3PW91 agrees most closely with gas-phase experimental data for BF_3 and also with MP2 calculations of the BF_3-localized modes in the complex; *m*PW1PW91 and B3LYP agree nearly as well. However, despite the effectiveness of DFT for structure, dipole moment, and vibrational frequencies, all DFT methods fail to predict a binding energy that compares favorably to the MCG3//MC-QCISD result of −5.7 kcal/mol.

I. Introduction

Numerous studies throughout the past decade have examined the ability of density functional theory (DFT)[1] to predict the structural and energetic properties of molecular complexes, including van der Waals,[2−7] hydrogen-bonded,[2,3,5,8−11] and donor−acceptor systems.[12−16] In particular, the latter have proven to be quite challenging, and in general, DFT has produced mixed results. Not surprisingly, most shortcomings arise when dispersion forces comprise a significant portion of the total interaction energy as DFT fails to account for it in any formal sense.[1] Most often, hybrid HF/DFT methods have performed better for complexes than have "pure" DFT methods.[4,7,12−16]

Boron−nitrogen complexes are the classic donor acceptor systems, and very recently it was found that pure methods (PBEPBE and PW91PW91) performed quite poorly compared to hybrid methods (MPW1K, *m*PW1PW91, B3PW91, and B3LYP) for amine−borane complexes.[16] Furthermore, it was noted that the very popular B3LYP method performed somewhat poorly compared to MPW1K and *m*PW1PW91.[16]

Our present interest is nitrile−BF_3 systems. Previously, it was noted that B3LYP and MP2 gave very consistent results

* Corresponding author phone: (715)836-5399; fax: (715)836-4979; e-mail: phillija@uwec.edu.
† University of Wisconsin−Eau Claire.
‡ University of Minnesota.

10.1021/ct0501248 CCC: $30.25
Published on Web 06/30/2005

for CH_3CN-BF_3.[17] However, upon proceeding to singly halogenated derivates of this complex (e.g. FCH_2CN-BF_3), B3LYP calculations yielded long B−N bonds (∼2.5 Å), indicative of fairly weak interactions. Given this, and the shortcomings of B3LYP noted in ref 16, we turned to other methods seeking some level of consistency. Unfortunately, we found considerable inconsistency, and moreover, no experimental gas-phase structures were available for these halo−acetonitrile complexes, making validation a difficult task.

In search of an appropriate test system, we turned to $HCN-BF_3$, a similar complex for which an experimental gas-phase structure[18] and dipole moment[19] have been published. The gas-phase B−N distance of 2.473(29) Å is quite similar to those we have calculated for the $X-CH_2CN-BF_3$ species using B3LYP. Furthermore, it is just shorter than the sum of the B and N van der Waals radii, and, as is true for its homologue CH_3CN-BF_3,[17,20,21] the structural properties of $HCN-BF_3$ are very sensitive to chemical environment.[20] For example, the solid-state structure has a B−N distance of 1.638(2) Å and an N−B−F angle of 105.6°.[22] Indeed, adding a single HCN molecule to form $(HCN)_2-BF_3$ causes the B−N distance to contract by 0.17 Å to 2.299(28) Å.[23]

Naturally, these remarkable structural properties have drawn the interest of theoreticians, though prior studies have been mainly concerned with issues secondary to our present interest, such as modeling the dative bond reaction path[24] or examining larger clusters (i.e. $(HCN-BF_3)_n$) in order to evaluate a cooperative mechanism for the large gas−solid structural difference.[25−27] Nevertheless, many equilibrium structures of $HCN-BF_3$ have been obtained in the process. Earlier studies yielded several MP2 results with B−N distances of 2.444 Å[25] and 2.443 Å[28] with the 6-31G** basis set, 2.296 with the D95** basis set,[26] 2.439 with the 6-31++G** basis set,[26] and 2.274 with the d95v++-(2d1f,2p) basis set.[24] Of these, only the 6-31++G** and 6-31G** results agree particularly well with experiment, although the d95v++(2d1f,2p) distance does increase to 2.510 Å after accounting for basis set superposition error.[24] Very recently, the structure was calculated with the MP2, B3LYP, MPW1K, and *m*PWPW91 methods using basis sets up to 6-311+G(d),[27] and the B−N distances obtained were 2.435 Å, 2.483, 1.882, and 2.296 Å, respectively. Clearly, the MP2 and B3LYP results are fairly consistent and agree fairly well with experiment, while the preferred methods for the amine−borane systems[16] do *much* more poorly. It is also worth noting that the MPW1K/6-311G(d) distance is 2.285 Å, indicating a peculiar sensitivity to diffuse functions, similar to that observed previously for CH_3CN-BF_3[17] using MP2 and B3LYP.

Our goal is straightforward; we seek an efficient and accurate DFT method for modeling the structures, binding energies, and vibrational frequencies of nitrile−BF_3 complexes such as $HCN-BF_3$. Below we present results from 12 different DFT methods and the MP2 level with large, triple-ζ basis sets (cc-pVTZ and aug-cc-pVTZ).[1] In addition, we report results from the multicoefficient correlation methods MC-QCISD[29] and MCG3,[30] in which high-level correlation energies are obtained from a scaled, additive approach. In general, such methods have yielded energetic predictions that are quite accurate.[1,29,30] Overall, we find that several hybrid DFT methods perform adequately with respect to the prediction of structure, dipole moment, and vibrational frequencies, but that all DFT methods fail to predict the binding energy accurately compared to the MC-QCISD and MCG3 results.

II. Computational Methods

MP2 and DFT calculations were performed using Gaussian03[31] version b.0.1 for all methods except O3LYP, for which version c.0.3 was used. For optimizations, all geometries were constrained to C_{3v} symmetry, and convergence criteria were set using the "opt=tight" option, which sets the maximum and RMS forces to 1.5×10^{-5} and 1.0×10^{-5} hartrees/bohr, respectively, and the maximum and RMS displacements to 6.0×10^{-5} and 4.0×10^{-5} bohr, respectively. An ultrafine grid was employed for all DFT calculations. The cc-pVTZ and aug-cc-pVTZ basis sets[1] were used almost exclusively, but for one method (B3PW91), the analogous double-ζ and quadruple-ζ basis sets were used to examine convergence behavior. Multi-Coefficient Gaussian-3 (MCG3)[30] energies as well as Multi-Coefficient Quadratic Configuration Interaction (MC-QCISD)[29] geometries and energies were obtained using MULTILEVEL version 4.0.[32] The maximum force criterion for MC-QCISD optimizations in MULTILEVEL was set to 1.0×10^{-4} hartrees/bohr.

To facilitate a direct comparison between computational (equilibrium) and experimental (vibrationally averaged) B−N distances, we calculated B−N potential curves using B3PW91, MP2, and MCG3 and solved the relevant one-dimensional Schrödinger equation to obtain wave functions and energies as well as vibrationally averaged bond lengths and dipole moments as expectation values over the B−N stretching coordinate. B3PW91 and MP2 potentials were calculated by freezing the B−N distance at 0.1 Å intervals from 1.6 to 3.6 Å and at 0.2 Å intervals from 3.6 to 4.0 Å and optimizing the geometry with respect to all remaining internal coordinates. MCG3 energies were then calculated for all MP2 geometries and for comparison a few B3PW91 geometries as well. Vibrational wave functions, energy levels, and average B−N distances were obtained using the FGHEVEN program,[33] which utilizes the Fourier Grid Hamiltonian method[34] to solve a one-dimensional Schrödinger equation for an arbitrary potential. To obtain the potential functions needed for FHGEVEN, we fit each potential to a pair of polynomial functions, fifth order for the points from 1.6 to 2.4 Å and fourth order for points from 2.4 to 4.0 Å. These functions reproduced the calculated energies along the curve to within about 1×10^{-5} hartrees. We considered different options for the reduced mass value in these calculations. Treating the system as a pseudodiatomic molecule, in which the individual atoms of the BF_3 and HCN subunits move coherently with one another throughout a vibrational period of the B−N stretching mode, one might estimate the reduced mass by simply taking the product of the HCN and BF_3 masses and dividing by their sum. Doing so results in a value of 19.25 amu. We compared this to the value used by

Gaussian for the B−N stretching mode in the MP2/aug-cc-pVTZ frequency calculation and found the latter to be much lower (10.16 amu). The difference derives from a coupling of the BF_3 umbrella mode and the B−N stretch. The displacement vectors for the ν_1 mode (predominantly B−N stretch, see below) in the Gaussian output indicate that the F atoms move much less along the B−N bond axis (∼60% relative amplitude) than does the B atom. This is not surprising, since the optimum N−B−F angle does change with B−N distance. Nevertheless it does complicate the use of a simplified one-dimensional model for the B−N stretching motion. In the end, we ran FGHEVEN with both mass values (19.25 and 10.16 amu) and found that there was no significant effect on the vibrationally averaged bond lengths or the qualitative features of the wave functions, despite the significant differences in the energy values. In any event, we note that the results shown below are those obtained with the reduced mass set to 10.16 amu.

III. Results and Discussion

The geometry of the complex is depicted in Figure 1 and calculated values of the B−N distance and N−B−F angle are displayed in Table 1, as are dipole moments and binding energies ($\Delta E = E^{\text{elec}}_{\text{HCN}-\text{BF}_3} - (E^{\text{elec}}_{\text{HCN}} + E^{\text{elec}}_{\text{BF}_3})$). The experimentally determined B−N distance[18] and dipole moment[19] are also listed for reference. The difference between the experimental (vibrationally averaged) and theoretical (equilibrium) B−N distances are also included in Table 1 (ΔR), and values for DFT/aug-cc-pVTZ methods that differ from the experimental value by less than 0.1 Å are noted in bold.

Structure and B−N Distance Potential. For comparisons of structural results, we focus initially on the B−N distance, as other structural parameters such as the N−B−F angle track it systematically, and for that matter it dominates the experimental moment of inertia.[18] In fact, the N−B−F angle quoted in the experimental work reflects an average of experiment and theory, and the other parameters were left fixed at the monomer values in the structural analysis.[18]

As a whole, the structural results for $HCN-BF_3$ are much less consistent than those for the amine−borane systems.[16] Nevertheless, results from the various hybrid DFT methods are reasonably consistent and most yielded B−N distances around 2.5 Å. The notable exceptions are MPW1K, which gives a somewhat shorter result of 2.323 Å with the aug-cc-pVTZ basis set, and O3LYP, for which the distances are quite long, especially with the aug-cc-pVTZ basis set. Among the results that compare favorably to experiment, the aug-cc-pVTZ distances are systematically shorter than the cc-pVTZ values by 0.1−0.2 Å. A similar "diffuse function effect" was noted previously in ref 27 for MPW1K and also for CH_3CN-BF_3,[17] though it is much less pronounced in the present case. In contrast, pure DFT methods perform quite poorly, as most of the calculated B−N distances are longer than experiment, especially OLYP. The exception is *m*PWPW91, which agrees quite well; and like most of the hybrid DFT results, the bond length is a bit shorter for the aug-cc-pVTZ basis set. Interestingly, the MP2/aug-cc-pVTZ result is notably shorter than experiment, by about 0.1 Å, and we initially suspected a genuine difference between the equilibrium and vibrationally averaged structures, stemming from a flat B−N distance potential, which had been examined previously at the MP2/ d95v++(2d1f,2p) level.[24] However, the MC-QCISD result for R_{BN} is 2.472 Å, which is almost coincident with experiment.

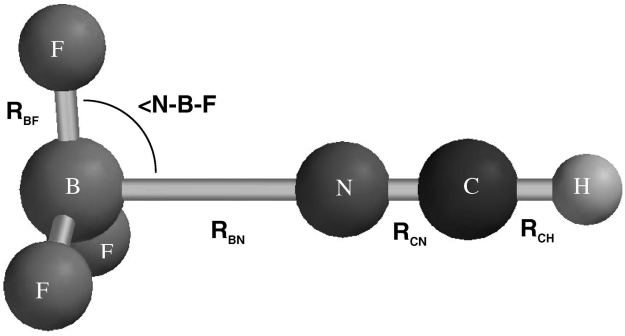

Figure 1. Structural parameters of $HCN-BF_3$.

The apparent inconsistency of the MP2 results relative to experiment and MC-QCISD, together with the very slight difference in MCG3 energies between the MP2 and MC-QCISD minima (0.2 kcal/mol), caused us to undertake a further examination of the intermolecular potential. Figure 2 shows B−N potential curves obtained via B3PW91, MP2, MCG3//B3PW91/aug-cc-pVTZ, and MCG3//MP2/aug-cc-pVTZ calculations. It is worth noting that the MCG3 energies of the B3PW91 (open circles in Figure 2) and MP2 geometries are very similar, within 0.05 kcal/mol in every instance. Indeed, the B3PW91 curve does have a slightly flattened region along the inner wall, around 2.0 Å, which is somewhat reminiscent of the CH_3CN-BF_3 potential, but is much less pronounced in this case. This feature is much less apparent in the MP2 and MCG3 curves.

Vibrational energy levels and wave functions for the B−N stretching mode (from the MCG3//MP2 curve) are shown in Figure 3. For the most part, these functions are quite symmetrical and do not reflect a great deal of anharmonicity. As a result, the average B−N bond distances calculated as expectation values over the vibrational wave functions differ only slightly from the equilibrium values. The results are included in Table 2 (below) with complete structural parameters for B3PW91, MP2, and MC-QCISD. At the B3PW91 level, the average distance is only 0.007 Å longer than the equilibrium distance. At the MP2 level, the average distance is actually 0.005 Å *shorter*. A comparison between the average bond length from the MCG3//MP2 potential curve and the optimized MC-QCISD structure is not entirely direct, but it is worth noting that the MCG3//MC-QCISD point does lie on the MCG3//MP2 curve in Figure 2. In any case, the equilibrium and average B−N distances agree exactly, and they differ from the measured value by only 0.001 Å (though the experimental error bar is actually much larger: 0.029 Å). We also note that the use of ground-state vibrational wave functions to compute the expectation value of R_{BN} is the appropriate choice, rather than a thermal average, since the experimental structure was deduced from an analysis of the microwave spectrum of the ground-state complex obtained in a cold, supersonic expansion.[18]

Table 1: Structural Properties, Dipole Moment, and Binding Energy of $HCN-BF_3$

method[a]	basis set	R_{BN} (Å)	ΔR (calc-exp)	⟨NBF (deg)	μ (D)	ΔE (kcal/mol)
HF	cc-pVTZ	2.675	0.202	92.2	4.17	
	aug-cc-pVTZ	2.664	0.191	92.3	4.22	−4.9
MP2	cc-pVTZ	2.419	−0.054	93.5	4.44	
	aug-cc-pVTZ	2.361	−0.112	93.9	4.51	−6.3
			Hybrid DFT Methods			
B3LYP	cc-pVTZ	2.552	0.079	92.8	4.14	
	aug-cc-pVTZ	2.535	**0.062**	93.0	4.23	−3.8
MPW1K	cc-pVTZ	2.352	−0.121	94.1	4.62	
	aug-cc-pVTZ	2.323	−0.150	94.4	4.74	−4.7
O3LYP	cc-pVTZ	2.596	0.123	91.4	3.58	
	aug-cc-pVTZ	2.996	0.523	91.4	3.61	−2.2
B3PW91	cc-pVTZ	2.493	0.020	93.2	4.26	
	aug-cc-pVTZ	2.465	**−0.008**	93.5	4.37	−3.2
*m*PW1PW91	cc-pVTZ	2.422	−0.051	93.6	4.41	
	aug-cc-pVTZ	2.390	−0.083	93.9	4.54	−4.1
B98	cc-pVTZ	2.539	0.066	92.9	4.17	
	aug-cc-pVTZ	2.513	**0.040**	93.1	4.28	−4.3
B97−2	cc-pVTZ	2.599	0.126	92.6	4.06	
	aug-cc-pVTZ	2.586	0.113	92.7	4.13	−3.3
			Pure DFT Methods			
BLYP	cc-pVTZ	2.655	0.182	92.4	3.93	
	aug-cc-pVTZ	2.642	0.169	92.5	4.02	−7.4
OLYP	cc-pVTZ	3.132	0.659	91.1	3.39	
	aug-cc-pVTZ	3.203	0.730	91.0	3.43	−1.8
BPW91	cc-pVTZ	2.597	0.124	92.7	4.02	
	aug-cc-pVTZ	2.655	0.182	93.0	4.13	−2.3
*m*PWPW91	cc-pVTZ	2.503	0.030	93.2	4.18	
	aug-cc-pVTZ	2.467	**−0.006**	93.5	4.32	−3.5
HCTH	cc-pVTZ	2.896	0.423	91.5	3.60	
	aug-cc-pVTZ	2.922	0.449	91.5	3.64	−3.4
			Multicoefficient Methods			
MC-QCISD[b]		2.472	−0.001	92.9		−5.6
MCG3[c]//MCQISD						−5.7
MC-QCISD//MP2						−5.5
MCG3//MP2						−5.6
experiment[q]		2.473(29)			4.135(7)	

[a] See ref 1. [b] Reference 29. [c] Reference 30. [d] References 18 and 19.

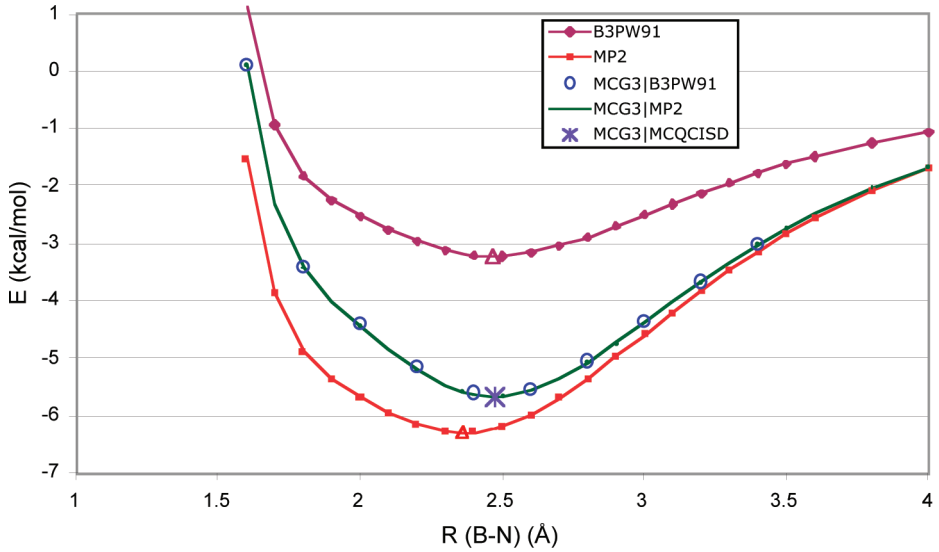

Figure 2. The B−N distance potential of $HCN-BF_3$. The zero of energy is set to that of the infinitely separated monomers. The aug-cc-pVTZ basis set was used for the B3PW91 and MP2 calculations. Minimum energy points on the MP2 and B3PW91 curves are noted with open triangles.

Thus, it appears that a comparison of equilibrium and vibrationally averaged structures is valid for this system, and we conclude that the best DFT methods for structure prediction seem to be the hybrid methods B3PW91 and B98 as well as the pure method *m*PWPW91. As such, we tested for convergence of the structural results by calculating B3PW91 structures with the cc-pVDZ, aug-cc-pVDZ, cc-pVQZ, and aug-cc-pVQZ basis sets. The B−N distances obtained were 2.312 Å, 2.305 Å, 2.504 Å, and 2.494 Å, respectively. Thus, the structure is nearly converged at the aug-cc-pVTZ level, but the B−N distance may indeed be a bit longer at the infinite basis set limit.

Complete structural results for B3PW91/aug-cc-pVTZ, MP2/aug-cc-pVTZ, and MC-QCISD (which includes the

Table 2: Experimental and Theoretical Values of Structural Parameters for HCN−BF_3

method	R_{BN}(eq) (Å)	$\langle R_{BN}\rangle$ (Å)	R_{CN} (Å)	R_{BF} (Å)	R_{CH} (Å)	<N−B−F (deg)
B3PW91/aug-cc-pVTZ	2.465	2.472	1.143	1.319	1.068	93.5
MP2/aug-cc-pVTZ	2.361	2.356	1.164	1.324	1.107	93.9
MC-QCISD[a]	2.472	2.472	1.155	1.317	1.069	93.0
experiment[b]		2.473(29)	1.153	1.310	1.065	90−93

[a] The equilibrium geometry was determined from an optimization via MC-QCISD. The average bond length $\langle R_{BN}\rangle$ was determined from the B−N distance potential calculated via MCG3 energies at the MP2 geometries. See text for discussion. [b] Note that in the experimental structure analysis, most of the parameters were fixed at the values of free HCN, and BF_3. Also, there was very little sensitivity to the N−B−F angle, so a value of 91.5° was chosen as it was an average of experiment and theory. See ref 18 for discussion.

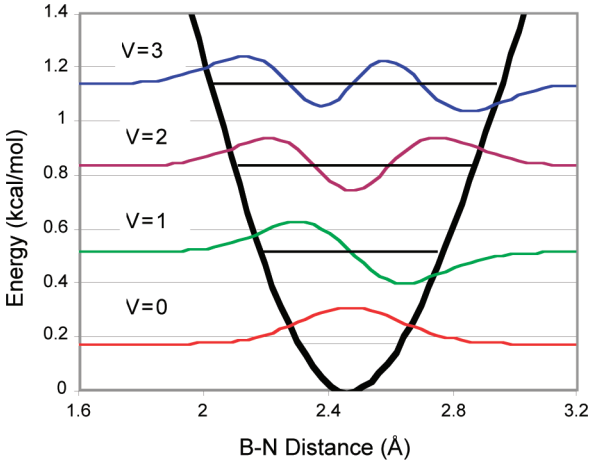

Figure 3. Energy levels and wave functions for the B−N stretching mode in HCN−BF_3.

$\langle R_{BN}\rangle$ value from the analysis of the MCG3//MP2 potential curve) as well as the experimental values[18] are provided in Table 2. It is worth noting that beyond the nonplanar distortion of the BF_3 unit, there are some other very minor structural changes that occur within the two monomer units upon complexation. Specifically, the B−F distance increases, and the C−N distance contracts. We note that the C−N distance in free HCN is calculated to be 1.167 Å by MP2/aug-cc-pVTZ and 1.146 Å by B3PW91/aug-cc-pVTZ, in both cases 0.003 Å longer than in the complex. Similarly, the B−F distances in free BF_3 are 1.317 and 1.314 Å for MP2/aug-cc-pVTZ and B3PW91/aug-cc-pVTZ, respectively, which is in both cases a bit shorter than in the complex. These complex-induced changes are quite small and indicate that the assumptions made in the experimental structural analysis were valid.

Dipole Moment. The dipole moment data in Table 1 demonstrate that the dipole increases monotonically with the B−N distance, as was noted previously in ref 27. In addition, it appears that this trend persists across all methods studied herein. This occurs because the nonplanar distortion of the BF_3 subunit increases with decreasing B−N and also because there is a steady increase in charge transfer as the bond shortens. Among methods that yield reasonable structures, all predict dipoles that are larger than experiment[19] by about 0.1−0.2 D. Furthermore, the MP2 results are much larger than experiment, consistent with the B−N distances being predicted to be too short. To determine whether this effect was structural or a result of method, we also calculated an MP2 dipole moment at the B3PW91 structure. The result, 4.40 D, is still significantly larger than the experimental dipole but only differs from the B3PW91 result by 0.03 D. We also considered the possibility that there might be a genuine difference between the experimental, vibrationally averaged dipole moment and the value that corresponds to the equilibrium bond length. Thus, using the vibrational wave functions determined from the analysis of the MCG3//MP2 potential, together with the dipole moment values for the points along the B3PW91/aug-cc-pVTZ curve, we calculated the expectation value of the dipole for the ground vibrational state. The dependence of the dipole moment on B−N distance is displayed in Figure 4, and since an analytical function was needed for the grid-based routine,[33] we fit the data from 1.7 to 3.6 Å to a fifth-order polynomial. This function reproduced the calculated dipole moment values to within about 0.01 D throughout the range of the fitted data (the average magnitude of the residuals was 0.0075 D). The vibrationally averaged dipole moment obtained in this analysis was 4.38 D, only 0.01 D larger than the equilibrium value of 4.37 D (for B3PW91 at 2.465 Å). The vibrationally averaged value is slightly larger because, about the average B−N distance (2.472 Å), the dipole moment function increases more rapidly toward shorter B−N distances than it decreases toward longer distances. It is also interesting to note that the point at which the dipole moment function

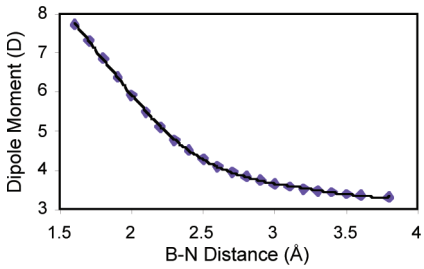

Figure 4. Calculated dipole moment (B3PW91/aug-cc-pVTZ) of HCN−BF_3 versus B−N distance.

Table 3: Observed and Calculated Frequencies[a] of BF_3

	mode[c]				
method[b]	ν_1 (SS)	ν_2 (SD)	ν_3 (AS)	ν_4 (AD)	RMS diff
experiment[d]	888	691	1449	480	
MP2	888	691	1463	475	**7.6**
B3LYP	885	681	1447	472	**6.3**
MPW1K	921	623	1509	460	49.3
O3LYP	877	676	1437	469	12.4
B3PW91	889	683	1457	473	**6.7**
*m*PW1PW91	896	686	1470	476	11.9
B98	890	683	1459	474	**7.0**
B97−2	888	685	1458	475	**6.0**
BLYP	851	658	1384	457	42.7
OLYP	851	658	1384	457	42.7
BPW91	856	660	1401	458	34.3
*m*PWPW91	858	660	1403	458	33.3
HCTH	862	669	1412	464	26.5

[a] In units of cm^{-1}. [b] The aug-cc-pVTZ basis set was used for all methods. [c] Modes 1−4 are the symmetric stretch (SS), the symmetric deformation (SD) (or "umbrella" mode), the asymmetric stretch (AS), and the asymmetric deformation (AD), respectively. [d] Reference 36.

Table 4: Calculated Vibrational Frequencies[a] of HCN−BF_3

mode no.	symmetry[b]	description	MP2[c]	B3LYP[c]	B3PW91[c]	*m*PW1PW91[c]
ν_1	A_1	BN stretch	98	87	77	79
ν_2	A_1	BF_3 "umbrella"	609	622	614	608
ν_3	A_1	BF symmetric stretch	870	873	874	878
ν_4	A_1	CN stretch	2055	2223	2230	2251
ν_5	A_1	CH stretch	3457	3440	3443	3461
ν_6	E	intermolecular bend	68	62	65	69
ν_7	E	BF_3/HCN wobble	201	162	177	194
ν_8	E	BF_3 asymmetric bend	474	471	472	475
ν_9	E	HCN bend	729	770	774	784
ν_{10}	E	BF_3 asymmetric stretch	1432	1424	1431	1438

[a] In units of cm^{-1}. [b] In the C_{3v} point group. [c] The aug-cc-pVTZ basis set was used for all methods.

begins to increase quite rapidly is very near the gas-phase B−N distance. A marked increase in charge separation would certainly impede further contraction of the B−N bond in the absence of a stabilizing medium of some form.

Binding Energy. The binding energy of the complex at the MCG3//MC-QCISD level is −5.7 kcal/mol. By contrast, all DFT methods compare quite poorly to MCG3//MC-QCISD as they predict binding energies that are smaller and indeed no closer to the MCG3 than the HF result. This is not surprising given that the complex is rather weak and DFT often fails in such instances.[1,11] Furthermore, the discrepancy must not stem from basis-set superposition error (BSSE), as the counterpoise correction typically reduces the value of the binding energy. The MP2 binding energy is slightly higher than MCG3, and therefore agreement with MCG3 could possibly be improved by correcting for BSSE. However, a counterpoise correction on the B3LYP/aug-cc-pVTZ structure of CH_3CN-BF_3 raised the energy by only 0.1 kcal/mol.[17]

Vibrational Frequencies. Experimental vibrational frequencies have provided key insight into the effects of bulk condensed phases on the structural properties of nitrile−BF_3 systems,[21] but gas-phase frequencies are needed for comparison, and we have relied on computations for these data in previous studies.[17] In this respect, there are two key criteria by which we judge model performance. First of all, a given model must adequately predict the gas-phase structure of the complex. In addition, since we have found that the BF_3-localized modes are most sensitive to structural changes,[17,21] modeling the BF_3 force field is key as well. Since gas-phase frequencies of HCN−BF_3 have not been measured (aside from the C−H stretch[35]), we turn to the frequencies of the BF_3 subunit. Table 3 displays observed[36] and calculated frequencies of BF_3, together with RMS differences between experiment and theory. We have *not* scaled these frequencies. Typically, computational frequencies are scaled by a factor slightly less than 1.0 to facilitate agreement with experiment[1] (e.g. 0.9806 for B3LYP/6-31G(d)[37]). In this instance, such a scaling would actually decrease agreement with experiment. A similar trend was noted previously in the study of CH_3-CN−BF_3 frequencies,[17] and therein it was (arbitrarily) decided to apply a scale factor only to frequencies above 2000 cm^{-1}, which only affected the CN and C−H stretches (of which the former seemed to be problematic, see below).

It is clear that, in addition to MP2, the hybrid methods B3LYP, B3PW91, B98, and B97-2 all perform quite well (RMS differences less than 10 cm^{-1}), and *m*PW1PW91 is nearly as good. Pure DFT methods perform quite poorly. For the complex, we selected three DFT methods that performed well on free BF_3 and bracketed the experimental structural results: B3LYP, B3PW91, and *m*PWPW91. These frequencies, together with MP2 data, are shown in Table 4. For the most part the results are consistent, especially for the BF_3-localized modes (ν_2, ν_3, ν_8, and ν_{10}). We note also that the differences among methods parallel those of the free BF_3 calculations, rather than the expected shifts based on the slight structural differences.[17] This most likely reflects the very small degree of nonplanar distortion in the BF_3 subunit. A few of the intermolecular modes are a bit higher for MP2, which reflects a tighter intermolecular potential (as is reflected in Figure 2). We also note that there is a significant difference between DFT and MP2 for the C−N stretch. The measured CN stretch of HCN is 2097 cm^{-1},[36] and we calculate 2021 cm^{-1} using MP2/aug-cc-pVTZ and 2204 cm^{-1} using B3PW91. Scaling the latter by a factor of 0.9772 (recommended for B3PW91/6-31G(d)[37]) would change the result to 2153 cm^{-1}, which is only a modest improvement. Thus, while DFT seems to do well for the BF_3 force field, it performs poorly for the HCN moiety, and the MP2 results are at best marginal.

IV. Conclusions

We have shown that certain hybrid DFT methods accurately predict the structure of HCN−BF_3 relative to experiment and demonstrated that calculated equilibrium structures can be compared to experimental, vibrationally averaged structures for this system. We also find that several hybrid DFT methods accurately predict the vibrational frequencies of BF_3 relative to experiment[36] and frequencies of the complex relative to MP2. The possible exception to this success is the CN stretching mode of the complex, for which the MP2 result also seems marginal. Overall, B3PW91 seems to perform the best when considering both structure and vibrational frequencies. We also found that both DFT and MP2 predict dipole moments that are quite reasonable, i.e., within about 0.2 D, of the experimental value. It was also demonstrated that the difference between the equilibrium and vibrationally averaged dipole moment values was negligible. However, despite their success with structure, frequencies, and dipole moment, all DFT methods significantly underestimated the complex binding energy, which was −5.7 kcal/mol at the MCG3//MC-QCISD level.

Acknowledgment. This work was supported by the National Science Foundation (RSEC CHE-0137438 and

CHE-0203346 to C.J.C. and CHE-0407824 to J.A.P.). J.A.P. also acknowledges The Henry Dreyfus Teacher-Scholar Program administered by the Camille and Henry Dreyfus Foundation as well as sabbatical support from the Faculty Sabbatical Leave Program administered by the Office of Research and Sponsored Programs at the University of Wisconsin—Eau Claire and the NSF-RSEC program at the University of Minnesota, Department of Chemistry.

References

(1) For a recent overview of DFT and other computational methods used and discussed herein, see: Cramer, C. J. *Essentials of Computational Chemistry*, 2nd ed.; John Wiley and Sons: Chichester, 2004; and references therein.

(2) Hobza, P.; Sponer, J.; Reschel, T. *J. Comput. Chem.* **1995**, *16*, 1315.

(3) Garcia, A.; Cruz, E. M.; Sarasola, C.; Uglade, J. M. *J. Mol. Struct. (THEOCHEM)* **1997**, *397*, 191.

(4) Couronne, O.; Ellinger, Y. *Chem. Phys. Lett.* **1999**, *306*, 71.

(5) Tsuzuki, S.; Lüthi, H. P. *J. Chem. Phys.* **2001**, *114*, 949.

(6) Salazar, M. C.; Paz, J. L.; Hernandez, A. J.; Manzanares, C. I.; Ludena, E. V. *Theor. Chem. Acc.* **2001**, *106*, 218.

(7) Salazar, M. C.; Paz, J. L.; Hernandez, A. J.; Manzanares, C. I.; Ludena, E. V. *Int. J. Quantum Chem.* **2003**, *95*, 177.

(8) Kim, K.; Jordan, K. D. *J. Phys. Chem.* **1994**, *98*, 10089.

(9) Latajka, Z.; Bouteiller, Y. *J. Chem. Phys.* **1994**,*101*, 9793.

(10) Del Bene, J. E.; Person, W. B.; Szczpaniak, K. *J. Phys. Chem.* **1995**, *99*, 10705.

(11) Cybilski, S. M.; Seversen, C. E. *J. Chem. Phys.* **2005**, *122*, 014117.

(12) Ruiz, E.; Salahub, D. R.; Vela, A. *J. Am. Chem. Soc.* **1995**, *117*, 1141.

(13) Ruiz, E.; Salahub, D. R.; Vela, A. *J. Phys. Chem.* **1996**, *100*, 12265.

(14) Latajka, Z.; Berski; S. *J. Mol. Struct. (THEOCHEM)* **1996**, *371*, 11.

(15) Garcia, A.; Cruz, E. M.; Sarasola, C.; Ugalde, J. M. *J. Phys. Chem. A* **1997**, *101*, 3021.

(16) Gilbert, T. M. *J. Phys. Chem. A* **2004**, *108*, 2550.

(17) Giesen, D. J.; Phillips, J. A. *J. Phys Chem. A* **2003**, *107*, 4009.

(18) Reeve, S. W.; Burns, W. A.; Lovas, F. J.; Suenram, R. D.; Leopold, K. R. *J. Phys. Chem.* **1993**, *97*, 10630.

(19) Fiacco, D. L.; Mo, Y.; Hunt, S. W.; Ott, M. E.; Roberts, A.; Leopold, K. R. *J. Phys. Chem. A* **2001**, *105*, 484.

(20) Leopold, K. R.; Canagaratna, M.; Phillips, J. A. *Acc. Chem. Res.* **1997**, *30*, 57, and references therein.

(21) Wells, N. P.; Phillips, J. A. *J. Phys. Chem. A* **2002**, *106*, 1518.

(22) Burns, W. A.; Leopold, K. R. *J. Am. Chem. Soc.* **1993**, *115*, 11622.

(23) Fiacco, D. L.; Leopold, K. R. *J. Phys. Chem. A* **2003**, *107*, 2808.

(24) Hankinson, D. J.; Amlöf, J.; Leopold, K. R. *J. Phys. Chem.* **1996**, *100*, 6904.

(25) Iglesias, E.; Sordo, T. L.; Sordo, J. A. *Chem. Phys. Lett.* **1996**, *248*, 179.

(26) Cabaleiro-Lago, E. M.; Ríos, M. A. *Chem Phys. Lett.* **1998**, *294*, 272.

(27) Venter, G.; Dillen, J. *J. Phys. Chem. A* **2004**, *108*, 8378.

(28) Nxumalo, L. M.; Andrezejak, M.; Ford, T. A. *J. Chem. Inf. Comput. Sci.* **1996**, *36*, 377.

(29) Fast, P. L.; Truhlar, D. G. *J. Phys. Chem. A* **2000**, *104*, 6111.

(30) Tratz, C. M.; Fast, P. L.; Truhlar, D. G. *PhysChemComm* **1999**, 2/14, 1.

(31) Frisch, M. J.; Trucks, G. W.; Schlegel, H. B.; Scuseria, G. E.; Robb, M. A.; Cheeseman, J. R.; Montgomery, J. A., Jr.; Vreven, T.; Kudin, K. N.; Burant, J. C.; Millam, J. M.; Iyengar, S. S.; Tomasi, J.; Barone, V.; Mennucci, B.; Cossi, M.; Scalmani, G.; Rega, N.; Petersson, G. A.; Nakatsuji, H.; Hada, M.; Ehara, M.; Toyota, K.; Fukuda, R.; Hasegawa, J.; Ishida, M.; Nakajima, T.; Honda, Y.; Kitao, O.; Nakai, H.; Klene, M.; Li, X.; Knox, J. E.; Hratchian, H. P.; Cross, J. B.; Adamo, C.; Jaramillo, J.; Gomperts, R.; Stratmann, R. E.; Yazyev, O.; Austin, A. J.; Cammi, R.; Pomelli, C.; Ochterski, J. W.; Ayala, P. Y.; Morokuma, K.; Voth, G. A.; Salvador, P.; Dannenberg, J. J.; Zakrzewski, V. G.; Dapprich, S.; Daniels, A. D.; Strain, M. C.; Sarkas, O. F.; Malick, D. K.; Rabuck, A. D.; Raghavachari, K.; Foresman, J. B.; Ortiz, J. V.; Cui, Q.; Baboul, A. G.; Clifford, S.; Cioslowski, J.; Stefanov, B. B.; Liu, G.; Liashenko, A.; Piskorz, P.; Komaromi, I.; Martin, R. L.; Fox, D. J.; Keith, T.; Al-Laham; M. A.; Peng, C. Y.; Nanayakkara, A.; Challacombe, M.; Gill, P. M. W.; Johnson, B.; Chen, W.; Wong, M. W.; Gonzalez, C.; Pople, J. A. Gaussian, Inc., Pittsburgh, PA, 2003.

(32) MULTILEVEL-version 4.0/G03, by Rodgers, J. M.; Lynch, B. J.; Fast, P. L.; Zhao, Y.; Pu, J.; Chuang, Y.-Y.; Truhlar, D. G. University of Minnesota, Minneapolis, 2002, based on GAUSSIAN03, ref 31.

(33) http://www.tlchm.bris.ac.uk/dynamics/fghqcpe.for, accessed April, 2005.

(34) (a) Marston, C. C.; Balint-Kurti, G. G. *J. Chem. Phys.* **1989**, *91*, 3571. (b) Balint-Kurti, G. G.; Dixon, R. N.; Marston, C. C. *Intl. Rev. Phys. Chem.* **1992**, *11*, 317.

(35) Kerstel, E. R. Th.; Pate, B. H.; Mentel, T. F; Scoles, G. *J. Chem. Phys.* **1994**, *101*, 2762.

(36) Herzberg, G. *Molecular Spectra and Molecular Structure, Volume II, Infrared and Raman Spectra of Polyatomic Molecules*; Krieger Publishing Co.: Malabar, FL, 1991.

(37) Lynch, B. J.; Zhao, Y.; Truhlar, D. G. http:/comp.chem.umn.edu/database/freq_scale.htm, accessed April, 2005.

CT0501248